The Journal of Immunology

Identification of a Cytoplasmic Region of CD20 Required for Its Redistribution to a Detergent-Insoluble Membrane Compartment

Maria J. Polyak, Sweta H. Tailor and Julie P. Deans

J Immunol 1998; 161:3242-3248; ;
http://www.jimmunol.org/content/161/7/3242

The Journal of Immunology is published twice each month by
The American Association of Immunologists, Inc.,
1451 Rockville Pike, Suite 650, Rockville, MD 20852

Print ISSN: 0022-1767 Online ISSN: 1550-6606.

Identification of a Cytoplasmic Region of CD20 Required for Its Redistribution to a Detergent-Insoluble Membrane Compartment[1]

Maria J. Polyak, Sweta H. Tailor, and Julie P. Deans[2]

CD20 is a B lymphocyte integral membrane protein with signal-transducing properties. Abs directed toward extracellular CD20 epitopes activate nonreceptor tyrosine kinases and modulate cell cycle progression of B lymphocytes. Recently, we demonstrated that binding of CD20 Abs to B cells induces the rapid redistribution of up to 95% of CD20 molecules to low density, detergent-insoluble membrane microdomains and induces the appearance of an approximately 50-kDa tyrosine-phosphorylated protein in the same compartment. Active relocalization of CD20 may thus be critical to the initiation of signaling events by CD20. The CD20 cDNA sequence predicts a nonglycosylated protein with four transmembrane-spanning regions and intracellular amino and carboxyl termini. Here we provide verification of the location of both the intracellular and extracellular regions of the CD20 molecule and identify a membrane-proximal sequence in the cytoplasmic carboxyl tail that is required for CD20 to redistribute to detergent-insoluble membrane microdomains. ***The Journal of Immunology,*** **1998, 161: 3242–3248.**

CD20 is a B cell molecule capable of transducing cell cycle progression signals in resting B cells upon Ab ligation (1–5). Recently, we demonstrated that Ab binding to the CD20 extracellular domain causes rapid redistribution of a large majority of CD20 molecules to a low density, detergent-insoluble plasma membrane compartment (6). In many cell types this compartment includes caveolae, microinvaginations in the plasma membrane where Src family tyrosine kinases, G protein-coupled receptors, GPI[3]-linked proteins, calcium channels, and ATPases, are found (7, 8). Although there is an apparent absence of caveolae in lymphocytes, biochemically similar structures can be isolated, sometimes referred to as rafts or DIGS (detergent-insoluble glycolipid-enriched structures) (9, 10). These microdomains are estimated to contain <1% of membrane proteins and, like caveolae, are enriched in a variety of proteins involved in signal transduction, including Src family tyrosine kinases, multiple heterotrimeric G proteins, and GPI-linked proteins (8). We have proposed that active relocalization of CD20 into these microdomains is a necessary event in the initiation of CD20 signaling, and in support of this, we find that an activating anti-CD20 mAb uniquely induces the appearance of a tyrosine-phosphorylated protein of about 50 kDa in the same compartment (6). There are only a few reports in the current literature of active relocalization of cell surface molecules into or out of detergent-insoluble domains or caveolae (11–16), and there is no information yet on the mechanism(s) that controls their redistribution. CD20 provides an excellent model for investigating the mechanisms involved in redistribution, since it is completely excluded from detergent-insoluble domains in the resting state and can be easily and massively induced to translocate into them upon Ab binding (6).

Human CD20 and its murine equivalent, Ly-44, have been cloned, and their genetic sequences have been characterized (17–20). Based on hydrophobicity data and the lack of a signal sequence, CD20 is predicted to have intracellular N- and C-termini, four transmembrane spans (TM1–4), and an extracellular domain between TM3 and TM4 (18, 19). We sought to dissect the cytoplasmic regions of CD20 in search of sequences involved in controlling its redistribution. However, since signal sequences are not always necessary for extracellular localization of N-terminal regions (21–26), the predicted membrane orientation of CD20 required confirmation.

In this study Abs generated against peptides in the N- and C-terminal regions of CD20 were used to determine its membrane orientation. Then, deletion mutants of intracellular regions were generated and examined to determine their effects on the redistribution of CD20 to Triton-insoluble membrane microdomains.

Materials and Methods

Cells and Abs

Raji lymphoblastoid B cells were grown in RPMI/5% FBS. Molt-4 T cells expressing transfected CD20 cDNA (27) were grown in RPMI/10% FBS in the presence of 0.4 mg/ml geneticin (Life Technologies, Gaithersburg, MD). CD20-specific 2H7 mAb was provided by Dr. J. Ledbetter (Bristol-Myers Squibb, Seattle, WA). Antisera against the amino and carboxyl regions of CD20 (herein named anti-CD20N and anti-CD20C) were generated by immunizing rabbits with either OVA-conjugated CD20N peptide (CD20N-P; residues 25–41, SGPKPLFRRMSSLVGPT) or OVA-conjugated CD20C peptide (CD20C-P; residues 231–245, SAEEKKEQTIEI KEE; peptides were provided by James Blake, Bristol-Myers Squibb). The Abs were affinity purified using the Pierce Sulfolink Kit (Rockford, IL).

Mutagenesis and transfections

The generation of the two truncation mutants used in this study, NΔ1–49 and CΔ253–297, were described previously (27). CΔ219–225,

Immunology Research Group, Department of Biochemistry and Molecular Biology, University of Calgary, Calgary, Alberta, Canada

Received for publication March 4, 1998. Accepted for publication May 26, 1998.

The costs of publication of this article were defrayed in part by the payment of page charges. This article must therefore be hereby marked *advertisement* in accordance with 18 U.S.C. Section 1734 solely to indicate this fact.

[1] This work was supported by grants from the Natural Sciences and Engineering Research Council of Canada and the National Cancer Institute of Canada with funds from the Terry Fox Run, by scholarship awards from the Alberta Heritage Foundation for Medical Research and the Medical Research Council of Canada (to J.D.), and by summer studentship awards from the Alberta Heritage Foundation for Medical Research (to S.T.).

[2] Address correspondence and reprint requests to Dr. Julie Deans, Department of Medical Biochemistry, University of Calgary, Health Sciences Center, 3330 Hospital Dr. NW, Calgary, Alberta, Canada T2N 4N1. E-mail address: jdeans@acs.ucalgary.ca

[3] Abbreviations used in this paper: GPI, glycosylphosphatidylinesitol; TM, transmembrane; CD20N-P, CD20N peptide.

0022-1767/98/$02.00

Table I. *PCR primers used in the preparation of CD20 derivatives*[a]

Designation	Primer	Sequence of Primer
C220A	5′	AAAAGAACGGCCTCCAGACCC
	3′	GGGTCTGGAGGCCGTTCTTTT
CΔ219-225	5′	TGGAAAAGAAACATAGTTCTCCTGTCA
	3′	AACTATGTTTCTTTTCCATTCATTCTC
CΔ226-252	5′	CCCAAATCTTCTTCCCAACCAAAGAAT
	3′	TTGGGAAGAAGATTTGGGTCTGGAGCA

[a] All sequences are written in the 5′ to 3′ direction.

CΔ226–252, and the Cys^{220}/Ala point mutation (C220A) were produced by overlap extension PCR (28) using the internal primer pairs shown in Table I and the CD20 cDNA template provided by Dr. Ivan Stamenkovic (Charleston, MA). Outside primers used were 5′-ATAATGAATTCATT GAGCCTCTTT-3′ (5′ primer that includes a unique *Eco*RI restriction site at position 451 of the CD20 cDNA) and 5′-AATCACTTAAG GAGAGCT-3′ (3′ primer that includes a unique *Afl*II site at position 983). The PCR fragments were digested with *Eco*RI and *Afl*II, then cloned into pBluescript containing a CD20 cDNA insert from which the *Eco*RI-*Afl*II fragment had been excised. The sequence of each construct was confirmed before subcloning into the BCMGSneo mammalian expression vector (29). Transfection into Molt-4 T cells and selection of geneticin-resistant clones, were performed as previously described (27).

Immunofluorescence

Cells were suspended and incubated in RPMI/5% FBS with anti-CD20 or control Abs, washed once, and resuspended in 100 μl (1/100) dilution of either FITC-conjugated rabbit anti-mouse IgG (Southern Biotechnology Associates, Birmingham, AL) or FITC-conjugated goat anti-rabbit IgG (ICN, Costa Mesa, CA) as appropriate. For intracellular staining, Raji B cells (1×10^6 cells/sample) were permeabilized with 0.05% saponin in RPMI/5% FBS for 30 min on ice. Subsequent Ab incubation and wash steps were performed as described above, except in the presence of 0.01% saponin. For the peptide inhibition studies, anti-CD20N and anti-CD20C Abs were preincubated with the immunizing peptides CD20N-P and CD20C-P, respectively, for 3 h at room temperature. Immunofluorescence of all samples was measured using a FACScan cytometer (Becton Dickinson, Mountain View, CA).

Trypsin and proteinase K digests

Raji cells (2×10^6/sample) were washed and resuspended in 50 mM Tris-HCl (pH 7.5), then incubated alone or with trypsin (0.2 μg/μl) for 15 min on ice. For proteinase K digests, Raji cells were washed and resuspended in PBS, then incubated alone or with 12.5 μM proteinase K for 15 min on ice. Protease inhibitors (4 mM Pefabloc (Boehringer Mannheim, Laval, Quebec), 1 μg/ml aprotinin, 1 μg/ml leupeptin, and 1 mM PMSF) were added to halt digestion. Samples were then rapidly centrifuged, and the supernatants were aspirated. Cell pellets were lysed directly in 2× sample buffer, heated to 100°C for 5 min, and loaded on 12.5% polyacrylamide gels (4×10^5 cell equivalents/lane).

Cell stimulation and sample preparation

Cells (5×10^6/sample) were washed in PBS, not treated or treated with 5 μg of 2H7 mAb at 37°C for 15 min, then pelleted and lysed in 20 mM Tris, pH 7.5, containing 0.5% Triton X-100, 1 μg/ml aprotinin, 1 μg/ml leupeptin, 5 mM EDTA, and 1 mM PMSF. After 15 min on ice, samples were centrifuged at 14,000 × *g* for 15 min at 4°C to pellet the insoluble material. Lysates were transferred to clean tubes and mixed with 2× SDS sample buffer. The insoluble pellets were washed four times with lysis buffer and then solubilized in 2× SDS sample buffer. Samples were heated to 100°C for 5 min before separation on 10% polyacrylamide gels ($1–3 \times 10^5$ cell equivalents of lysates/lane; 5×10^5 cell equivalents of pellets/lane). For immunoprecipitation, lysates from 10^7 cells were transferred to clean tubes, incubated overnight at 4°C with either normal rabbit serum or anti-CD20N antiserum (2 μl), then mixed with 20 μl of protein A-Sepharose (Repligen, Cambridge, MA) for 2 h. The Sepharose beads were washed three times with lysis buffer and once with PBS, and then mixed with 2× SDS sample buffer. Prestained m.w. markers (Life Technologies or New England Biolabs (Beverly, MA)) were run on each gel, and proteins were transferred to Immobilon P (Millipore, Bedford, MA) membranes for immunoblotting.

Immunoblots

Membranes were blocked overnight with 5% BSA, then incubated for 3 h with anti-CD20N or anti-CD20C Abs diluted in 1% BSA. After washing the membranes, bound Abs were detected with protein A-horseradish peroxidase (Bio-Rad, Richmond, CA). Proteins were visualized using chemiluminescence (Pierce) recorded on Kodak X-OMAT film (Eastman Kodak, Rochester, NY) For the peptide inhibition experiments, anti-CD20N and anti-CD20C Abs were incubated alone or with either CD20N-P or CD20C-P for 30 min on ice before immunoblotting.

Results and Discussion

Specificity of CD20N and CD20C Abs

To determine the membrane orientation of CD20, Abs against known epitopes were generated in rabbits by immunization with OVA-conjugated CD20 N and C region peptides. The resulting antisera, anti-CD20N and anti-CD20C, were affinity purified and tested for specificity before use in membrane orientation studies (Fig. 1). Specificity was confirmed in three ways. First, both antisera detected proteins of 33 to 35 kDa in immunoblots of whole cell lysates derived from Raji B cells (Fig. 1*A*). CD20 migrates on SDS-PAGE as a single band, a doublet, or a triplet depending upon the quantity of protein present and the resolving power of the gel. The differently migrating species are the result of differential serine/threonine phosphorylation (30). Preincubation of the Abs with the immunizing peptides inhibited binding, while incubation with irrelevant peptides did not (Fig. 1*A*). Second, immunoprecipitation with anti-CD20N and detection by immunoblotting with anti-CD20C demonstrated that both Abs recognized epitopes on the same protein (Fig. 1*B*). Third, both Abs specifically recognized CD20 ectopically expressed by transfection in the Molt-4 T cell line (Fig. 1*C*).

Confirmation of the membrane orientation of CD20

Localization of the N- and C-terminal regions of CD20 was assessed by indirect immunofluorescence using intact and membrane-permeabilized Raji B cells. CD20N and CD20C Abs did not recognize CD20 on intact cells (Fig. 2). However, after permeabilization there was a specific increase in intracellular staining by both anti-CD20N and anti-CD20C Abs that was prevented by preincubation of the Abs with immunizing peptide. Effective permeabilization of the cells was confirmed by the detection of the cytoplasmic Src family tyrosine kinase Lyn only after the permeabilization procedure (data not shown). Since the epitopes recognized by anti-CD20N and anti-CD20C were accessible only after permeabilization, these data confirm the intracellular location of both N- and C-terminal regions of CD20.

The intracellular location of both termini indicates that CD20 must assume one of three possible topologies relative to the plasma membrane (see Fig. 8*A*). Protease digestion of intact cells was performed to evaluate the number and the locations of extracellular

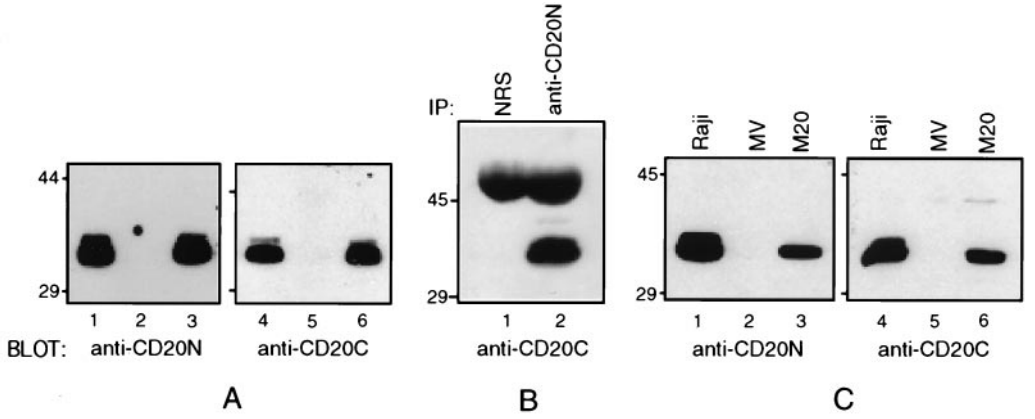

FIGURE 1. Specificity of anti-CD20N and anti-CD20C Abs for CD20. *A*, Whole cell lysate prepared from Raji B cells was separated on 10% SDS-PAGE and then immunoblotted with anti-CD20N or anti-CD20C Ab, either untreated (*lanes 1* and *4*) or previously incubated with immunizing peptide (*lanes 2* and *5*) or irrelevant peptide (*lanes 3* and *6*). *B*, Whole cell lysate prepared from Raji B cells was immunoprecipitated with either normal rabbit serum (NRS; *lane 1*) or anti-CD20N Ab (*lane 2*), separated on 10% SDS-PAGE, and then immunoblotted with anti-CD20C Ab. The bands above the 45-kDa marker are rabbit heavy chain. *C*, Whole cell lysates prepared from Raji B cells (*lanes 1* and *4*) or Molt-4 T cells transfected with either vector alone (MV; *lanes 2* and *5*) or CD20 cDNA (M20; *lanes 3* and *6*) were separated on 10% SDS-PAGE and then immunoblotted with anti-CD20N or anti-CD20C Ab.

loops. Complete digestion of extracellular regions would be expected to result in either 8- or 15-kDa N-terminal fragments depending on whether the polypeptide is exposed at the cell surface on the carboxyl side of TM1. For these studies we used both trypsin, which cuts specifically on the carboxylic acid side of arginine or lysine, and the nonspecific protease proteinase K to treat intact Raji B cells as described in *Materials and Methods*. There is no trypsin digest site present in the putative loop between TM1 and TM2, and four sites in the hydrophilic region between TM3 and TM4. Therefore, the presence of an extracellular TM1-TM2 loop (Fig. 8*A*, *ii*) would be expected to generate approximately 15- and 8-kDa N-terminal fragments by trypsin and proteinase K, respectively. Further, there are four trypsin sites in the short hydrophilic stretch between TM2 and TM3. These sites would only be exposed in the two transmembrane/one extracellular loop model (Fig. 8*A*, *i*) and would also generate a significantly larger trypsin fragment compared with proteinase K. The only topology that would generate 15-kDa fragments after digestion with either trypsin or proteinase K is shown in Figure 8*A*, *iii*.

The size of the smallest N-terminal fragment generated by digestion of intact cells with either trypsin or proteinase K was slightly >15 kDa (Fig. 3), indicating that the protein does not exit to the cell surface between TM1 and TM3, and that there is a single extracellular loop between TM3 and TM4 (Fig. 8*A*, *iii*). Recognition of more than one band in both the trypsin- and proteinase K-digested samples by CD20N Ab is probably due to serine/threonine phosphorylation as seen in the intact protein. Incomplete digestion by trypsin may account for the third and largest N-terminal fragment detected. Fragments obtained after proteinase K digestion were slightly smaller than that obtained after trypsin digestion, as expected due to clipping of a few extra residues between the most N-terminal trypsin cut site and the outer leaflet of the plasma membrane.

The size of the C-terminal fragments (~21 kDa) resulting from digestion by either trypsin or proteinase K significantly exceeded the expected size (14 kDa), but is too large to be accounted for by incomplete digestion of the extracellular loop. The discrepancy in size may be attributable to post-translational modifications in the C-terminal region, such as phosphorylation and/or acylation (dis-

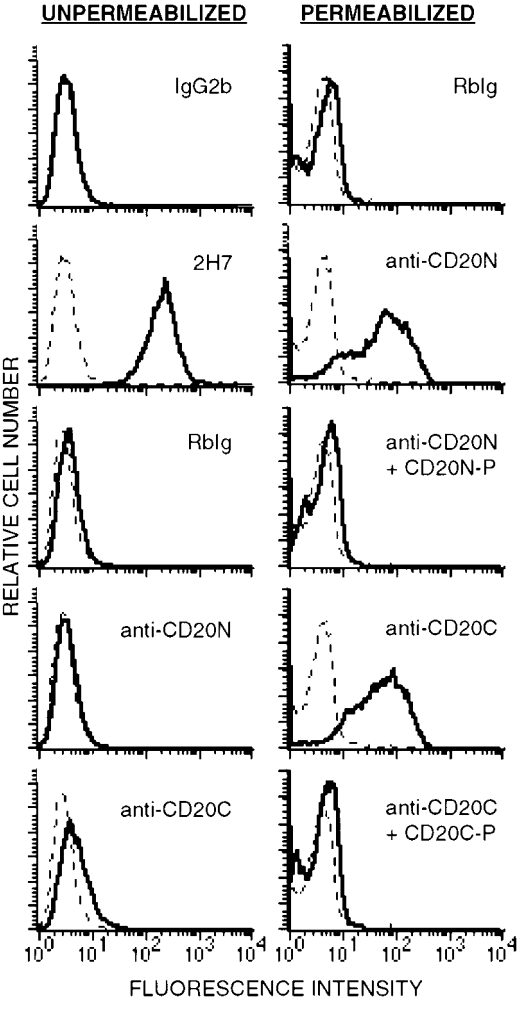

FIGURE 2. Anti-CD20N and anti-CD20P Abs recognize intracellular epitopes. Indirect immunofluorescence was performed on untreated and saponin-permeabilized Raji B cells. Dashed line profiles show binding of the FITC-labeled secondary Ab alone. Solid line profiles show binding of the primary Abs indicated.

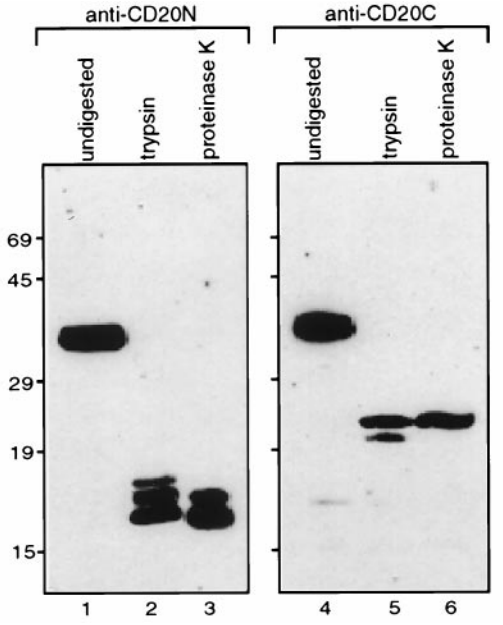

FIGURE 3. Trypsin and proteinase K digests of CD20. Raji B cells were either untreated (*lanes 1* and *4*) or digested with trypsin (*lanes 2* and *5*) or proteinase K (*lanes 3* and *6*) before lysis. Samples were separated on 12.5% SDS-PAGE and immunoblotted with anti-CD20N or anti-CD20C Ab as shown.

cussed further below), or to SDS-resistant protein-protein interactions occurring after digestion.

Since the epitopes recognized by anti-CD20N and anti-CD20C were not destroyed by protease digestion, these results, together with those in Figure 2, confirm their intracellular location. Data from extracellular protease digestion analyses support a four-TM domain topology with a single extracellular loop between TM3 and TM4, in agreement with the hydropathy prediction.

Generation of CD20 deletion mutants

We recently reported that CD20 redistributes from the soluble to the insoluble fraction of Triton X-100 cell lysates when B cells are exposed to Abs directed against extracellular epitopes of CD20 before lysis. The speed with which CD20 can be induced to translocate (6) indicates that the mechanism does not require de novo transcription or translation and suggests a conformational and/or post-translational change in the CD20 molecule. To identify regions that might be involved in the process of CD20 redistribution, we generated a series of cytoplasmic domain deletion mutants and tested them for their ability to translocate to the Triton-insoluble fraction following CD20 mAb engagement. Generation of a deletion construct that lacked the entire N-terminal cytoplasmic region (NΔ1–49) was described previously (27) and was detected in immunoblots using the polyclonal anti-CD20C Ab. As reported previously (27), deletion of the C-terminal region from either residue 215 or 222 to the end of the molecule at position 297 resulted in no or poor expression, respectively. However, internal deletions were expressed well (Fig. 4), and the C-terminal region was therefore analyzed using three constructs, CΔ219–225, CΔ226–252, and CΔ253–297, that were detected in immunoblots with the anti-CD20N Ab. All constructs were stably expressed in Molt-4 T cells, and expression levels were monitored by indirect immunofluorescence using the 2H7 mAb against an extracellular epitope (Fig. 4). Clones expressing either high or lower levels of wild-type CD20, as shown in Figure 4, were selected and used in different experiments to match the expression of the mutated forms of CD20 as closely as possible.

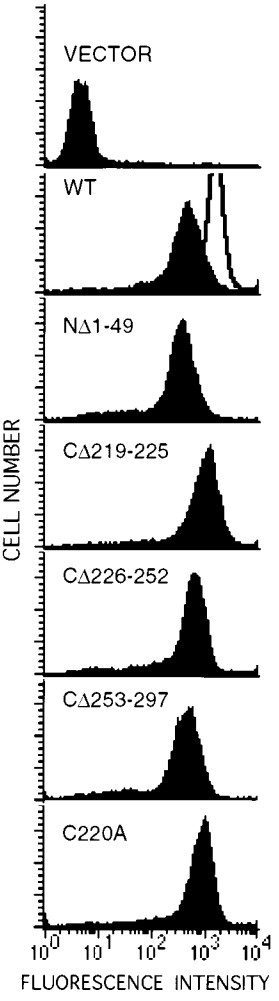

FIGURE 4. Expression of CD20 and derivatives on transfected Molt-4 T cells. All FACScan profiles show indirect immunofluorescence staining using 2H7 anti-CD20 mAb. In the case of the wild-type CD20-expressing cells, two clones were selected with different levels of expression (clear and black profiles).

Effects of cytoplasmic deletions on CD20 redistribution

Cells were incubated with or without 2H7 anti-CD20 mAb and lysed in Triton X-100-containing buffer, and both soluble and insoluble fractions were collected as described in *Materials and Methods*. The presence of CD20 in the soluble lysates or insoluble pellets was detected by immunoblot after SDS-PAGE, and the amounts were estimated by densitometry analysis of quadruplicate samples. In untreated cells, CD20 was always found entirely in the Triton-soluble fractions. As reported previously for CD20 on B cells, Ab-mediated ligation of wild-type CD20 in the transfected Molt-4 T cells induced virtually all CD20 protein to translocate to the insoluble compartment. This was observed both by the disappearance of CD20 from the soluble lysates and by its appearance in the insoluble pellets (Fig. 5). In contrast, a substantial amount of CD20 remained in the soluble compartment after Ab treatment when seven amino acids in the membrane-proximal region of the cytoplasmic C-terminal domain (CΔ219–225) were deleted (Fig. 5). The inhibition was not complete, however, as most clearly observed by the detection of some CD20 in the insoluble pellets.

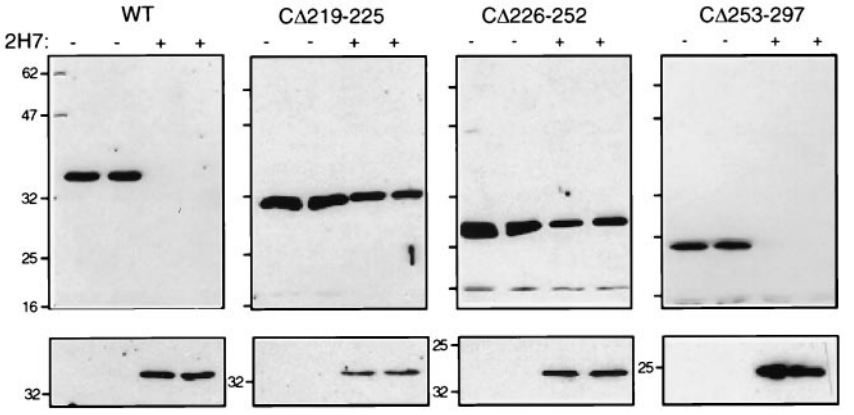

FIGURE 5. Effects of cytoplasmic C-terminal deletions on CD20 translocation. Anti-CD20N immunoblots of soluble lysates (*top panels*) or insoluble pellets (*bottom panels*) of duplicate samples of Molt-4 T cells expressing wild-type CD20 or deletion mutants as indicated, untreated (−) or treated for 15 min with 2H7 mAb (+) before lysis.

Densitometry analysis of quadruplicate samples estimated the degree of translocation to be about 25% compared with almost 100% for wild-type CD20. Deletion of an adjacent stretch of 26 residues (CΔ226–252) inhibited translocation also, albeit to a lesser extent (~75% translocated), whereas deletion of the C-terminal 45 residues (CΔ253–297) had no discernible effect on Ab-induced translocation. The CD20 mutant lacking the N-terminal region (NΔ1–49) was detected using the anti-CD20C polyclonal antiserum. This antiserum exhibited some background reactivity; nevertheless, it was clear in multiple experiments that the N-terminal deletion minimally reduced Ab-induced CD20 translocation by about 10% (Fig. 6).

Potential palmitoylation of Cys^{220} is not required for CD20 redistribution

The sequence 219 to 225 includes a cysteine residue at position 220 that is conserved in the other two members of the CD20 family of related proteins, i.e., FcERIβ and HTm4 (31, 32). The proximity of Cys^{220} to the inner leaflet of the plasma membrane makes it a potential site of reversible lipid modification by palmitoyl transferase. Palmitoylation is required for the caveolar localization of the Src family tyrosine kinase Hck and the endothelial nitric oxide synthase (33, 34), and is found on a number of other proteins in these microdomains, including several of the Gα signaling proteins and caveolin, a structural protein of caveolae. To determine whether a requirement for palmitoylation of Cys^{220} accounted for the inhibitory effect of the 219 to 225 deletion, alanine was substituted for cysteine at this position. Expression of C220A on transfected Molt-4 cells, as measured by indirect immunofluorescence, is shown in Figure 4. Mutation of Cys^{220} to alanine did not prevent or reduce Ab-induced translocation of CD20 to the insoluble pellet (Fig. 7), eliminating palmitoylation, or other potential modifications, of Cys^{220} as a mediator of CD20 redistribution. A second cytoplasmic cysteine is present in the loop between the second and third transmembrane regions; however, this cysteine is not conserved in FcERIβ, HTm4, or murine CD20, making it an unlikely candidate for an essential function. Since deletion of the internal loop prevented high level expression of CD20 (27), we could not detect the mutated protein in immunoblots and were unable to assess the impact of this deletion on CD20 translocation (data not shown).

Dynamic targeting of CD20 to detergent-insoluble domains is shown here to be dependent on a membrane-proximal sequence in the C-terminal cytoplasmic region (Fig. 8*B*). Although this region contains a potential palmitoylation site, this site was not required for the translocation of CD20. A similar observation was reported for caveolin; although palmitoylated, this modification is not required for caveolar localization of caveolin (35). Since multiple potential phosphorylation sites exist in both 219 to 225 and 226 to 252 sequences, it is possible that phosphorylation of CD20 is required for its translocation. CD20 is known to be phosphorylated (36, 37), and the level of phosphorylation is increased upon activation with phorbol esters (PMA) or Abs directed against surface IgM (37–40). The PMA-induced increase in phosphorylation of CD20 suggests that PKC may phosphorylate CD20 in vivo, as it does in vitro (39). Interestingly, however, we found that pretreatment of B cells

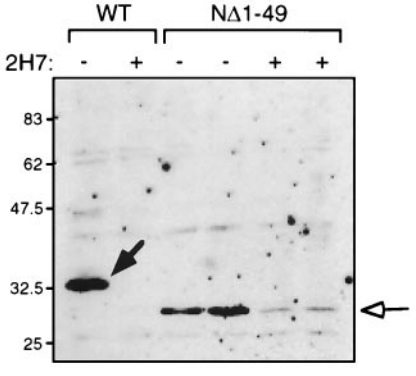

FIGURE 6. Effect of cytoplasmic N-terminal deletion on CD20 translocation. Anti-CD20C immunoblots of soluble lysates of duplicate samples of Molt-4 T cells expressing CD20 (WT; solid arrow) or N-terminal deletion mutant (NΔ1–49; clear arrow), untreated (−) or treated for 15 min with 2H7 mAb (+) before lysis.

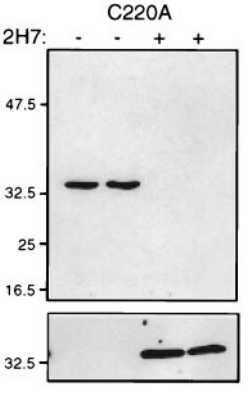

FIGURE 7. Mutation of Cys^{220} does not prevent CD20 translocation. Anti-CD20N immunoblots of soluble lysates (*top panel*) or insoluble pellets (*bottom panel*) of duplicate samples of Molt-4 T cells expressing a point mutation at Cys^{220}, untreated (−) or treated for 15 min with 2H7 mAb (+) before lysis.

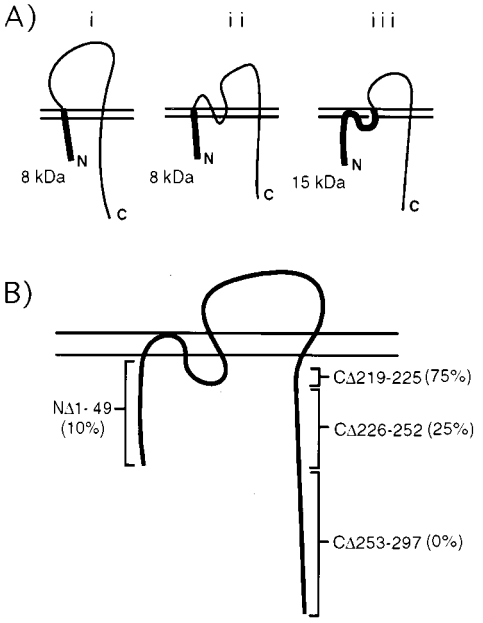

FIGURE 8. CD20 topology and regions affecting redistribution. *A*, Only three topologic orientations (*i–iii*) of CD20 are possible with intracellular N and C termini and a long hydrophilic stretch proximal to the most C-terminal transmembrane span. Complete digestion of extracellular regions would yield N-terminal fragments (bold lines) of the sizes indicated. Protease digestion data supports the topology shown in *iii*. *B*, The positions of the cytoplasmic deletions and the percent inhibition of CD20 redistribution are indicated.

with PMA does not promote, but rather inhibits, CD20 translocation (I. Popoff and J. Deans, unpublished observations). An alternate role for the identified translocation control region in CD20 may be its involvement in protein-protein interactions induced by a conformational change in CD20 upon Ab ligation. The putative interaction motif is likely to include sequence information spanning the 219 to 225 and 226 to 252 regions, and work is in progress in this laboratory to further define the boundaries of the region and to identify interacting proteins.

We speculate that the membrane-proximal sequence in the cytoplasmic C-terminal of CD20 may be involved in promoting oligomerization of CD20. Evidence from chemical cross-linking studies has supported the proposal that CD20 may exist as homodimers and -tetramers that could aggregate to form larger complexes (41). Interestingly, a membrane-proximal sequence in the cytoplasmic C-terminal of caveolin-1 has been shown to be involved in homotypic interactions that are thought to mediate the formation of caveolae (42, 43).

Only a few other examples of targeted redistribution of membrane receptors to caveolae or equivalent microdomains have been reported. The muscarinic acetylcholine receptor, the bradykinin receptor, and the protease receptor tissue factor are translocated into caveolae in response to agonists (11–16). GPI-linked proteins, which have also been implicated in signaling, become enriched in caveolae upon Ab cross-linking (44), and the high affinity receptor for IgE (FcERI), when aggregated, redistributes to detergent-resistant membrane domains (15, 16). There is currently no information, however, on the mechanisms underlying this phenomenon. CD20 shares significant sequence homology with the β subunit of the FcERI complex, particularly in regions corresponding to the membrane-spanning domains (32). Although Cys^{220} of CD20 is conserved in FcERIβ, the surrounding amino acids are not. The mechanism involved in localizing FcERIβ to detergent-insoluble microdomains may in any case be different, since it is released from the insoluble domains in concentrations of Triton X-100 $>$0.05% (16), whereas activated CD20 remains insoluble in 1% Triton X-100.

CD20 has been reported to mediate a number of biologic activities in B cells upon Ab engagement. It is likely that the redistribution of CD20 to insoluble membrane microdomains is a prerequisite event to the initiation of signaling and/or calcium channel formation. The identification of a cytoplasmic sequence that prevents CD20 redistribution is expected to lead to a full understanding of the underlying mechanism and perhaps to new insights into B cell activation.

Acknowledgments

We thank Dr. Steve Robbins and Ian Popoff for their comments on the manuscript, James Blake for providing OVA-conjugated CD20 peptides, and Dr. Jeff Ledbetter for the 2H7 mAb.

References

1. Smeland, E., T. Godal, E. Ruud, K. Beiske, S. Funderud, E. A. Clark, S. Pfeifer-Ohlsson, and R. Ohlsson. 1985. The specific induction of *myc* protooncogene expression in normal human B cells is not a sufficient event for acquisition of competence to proliferate. *Proc. Natl. Acad. Sci. USA 82:6255.*
2. Golay, J. T., E. A. Clark, and P. C. Beverley. 1985. The CD20 (Bp35) antigen is involved in activation of B cells from the G_0 to the G_1 phase of the cell cycle. *J. Immunol. 135:3795.*
3. Clark, E. A., G. Shu, and J. A. Ledbetter. 1985. Role of the Bp35 cell surface polypeptide in human B-cell activation. *Proc. Natl. Acad. Sci. USA 82:1766.*
4. Clark, E. A., G. Shu, and J. A. Ledbetter. 1986. Activation of human B cells mediated through two distinct cell surface differentiation antigens, BP35 and BP50. *Proc. Natl. Acad. Sci. USA 83:4494.*
5. Clark, E. A., and G. Shu. 1987. Activation of human B cell proliferation through surface Bp35 (CD20) polypeptides or immunoglobulin receptors. *J. Immunol. 138:720.*
6. Deans, J. P., S. R. Robbins, M. J. Polyak, and J. A. Savage. 1998. Rapid redistribution of CD20 to a low-density detergent-insoluble membrane compartment. *J. Biol. Chem. 273:344.*
7. Anderson, R. G. 1993. Caveolae: where incoming and outgoing messengers meet. *Proc. Natl. Acad. Sci. USA 90:10909.*
8. Lisanti, M. P., Z. Tang, P. E. Scherer, E. Kubler, A. J. Koleske, and M. Sargiacomo. 1995. Caveolae, transmembrane signalling and cellular transformation. *Mol. Membr. Biol. 12:121.*
9. Parton, R. G., and K. Simons. 1995. Digging into caveolae. *Science 269:1398.*
10. Simons, K., and E. Ikonen. 1997. Functional rafts in cell membranes. *Nature 387:589.*
11. Raposo, G., I. Dunia, C. Delavier-Klutchko, S. Kaveri, A. D. Strosberg, and E. L. Benedetti. 1989. Internalization of β-adrenergic receptor in A431 cells involves non-coated vesicles. *Eur. J. Cell Biol. 50:340.*
12. Feron, O., T. W. Smith, T. Michel, and R. A. Kelly. 1997. Dynamic targeting of the agonist-stimulated m2 muscarinic acetylcholine receptor to caveolae in cardiac myocytes. *J. Biol. Chem. 272:17744.*
13. de Weerd, W. F., and L. M. Leeb-Lundberg. 1997. Bradykinin sequesters B2 bradykinin receptors and the receptor-coupled Gα subunits $G\alpha_q$ and $G\alpha_i$ in caveolae in DDT1 MF-2 smooth muscle cells. *J. Biol. Chem. 272:17858.*
14. Sevinsky, J. R., L. V. Rao, and W. Ruf. 1996. Ligand-induced protease receptor translocation into caveolae: a mechanism for regulating cell surface proteolysis of the tissue factor-dependent coagulation pathway. *J. Cell Biol. 133:293.*
15. Field, K. A., D. Holowka, and B. Baird. 1995. Fc epsilon RI-mediated recruitment of p53/56^{lyn} to detergent-resistant membrane domains accompanies cellular signaling. *Proc. Natl. Acad. Sci. USA 92:9201.*
16. Field, K. A., D. Holowka, and B. Baird. 1997. Compartmentalized activation of the high affinity immunoglobulin E receptor within membrane domains. *J. Biol. Chem. 272:4276.*
17. Tedder, T. F., M. Streuli, S. F. Schlossman, and H. Saito. 1988. Isolation and structure of a cDNA encoding the B1 (CD20) cell-surface antigen of human B lymphocytes. *Proc. Natl. Acad. Sci. USA 85:208.*
18. Stamenkovic, I., and B. Seed. 1988. Analysis of two cDNA clones encoding the B lymphocyte antigen CD20 (B1, Bp35), a type III integral membrane protein. *J. Exp. Med. 167:1975.*
19. Einfeld, D. A., J. P. Brown, M. A. Valentine, E. A. Clark, and J. A. Ledbetter. 1988. Molecular cloning of the human B cell CD20 receptor predicts a hydrophobic protein with multiple transmembrane domains. *EMBO J. 7:711.*
20. Tedder, T. F., G. Klejman, C. M. Disteche, D. A. Adler, S. F. Schlossman, and H. Saito. 1988. Cloning of a complementary DNA encoding a new mouse B lymphocyte differentiation antigen, homologous to the human B1 (CD20) antigen, and localization of the gene to chromosome 19. *J. Immunol. 141:4388.*
21. Chen, H., and D. A. Kendall. 1995. Artificial transmembrane segments. Requirements for stop transfer and polypeptide orientation. *J. Biol. Chem. 270:14115.*

22. Denzer, A. J., C. E. Nabholz, and M. Spiess. 1995. Transmembrane orientation of signal-anchor proteins is affected by the folding state but not the size of the N-terminal domain. *EMBO J. 14:6311.*
23. Furman, I., O. Cook, J. Kasir, W. Low, and H. Rahamimoff. 1995. The putative amino-terminal signal peptide of the cloned rat brain Na^{+}-Ca^{2+} exchanger gene (RBE-1) is not mandatory for functional expression. *J. Biol. Chem. 270:19120.*
24. Kim, H., S. Paul, J. Gennity, J. Jennity, and M. Inouye. 1994. Reversible topology of a bifunctional transmembrane protein depends upon the charge balance around its transmembrane domain. *Mol. Microbiol. 11:819.*
25. Loo, T. W., C. Ho, and D. M. Clarke. 1995. Expression of a functionally active human renal sodium-calcium exchanger lacking a signal sequence. *J. Biol. Chem. 270:19345.*
26. Wong, E. F. S., S. K. Brar, H. Sesaki, C. Yang, and C. H. Siu. 1996. Molecular cloning and characterization of DdCAD-1, a Ca^{2+}-dependent cell-cell adhesion molecule, in *Dictyostelium discoideum. J. Biol. Chem. 271:16399.*
27. Deans, J. P., L. Kalt, J. A. Ledbetter, G. L. Schieven, J. B. Bolen, and P. Johnson. 1995. Association of 75/80-kDa phosphoproteins and the tyrosine kinases Lyn, Fyn, and Lck with the B cell molecule CD20: evidence against involvement of the cytoplasmic regions of CD20. *J. Biol. Chem. 270:22632.*
28. Horton, R. M., S. N. Ho, J. K. Pullen, H. D. Hunt, Z. Cai, and L. R. Pease. 1993. Gene splicing by overlap extension. *Methods Enzymol. 217:270.*
29. Karasuyama, H., A. Kudo, and F. Melchers. 1990. The proteins encoded by the VpreB and λ5 pre-B cell-specific genes can associate with each other and with mu heavy chain. *J. Exp. Med. 172:969.*
30. Tedder, T. F., G. McIntyre, and S. F. Schlossman. 1988. Heterogeneity in the B1 (CD20) cell surface molecule expressed by human B-lymphocytes. *Mol. Immunol. 25:1321.*
31. Adra, C. N., J. M. Lelias, H. Kobayashi, M. Kaghad, P. Morrison, J. D. Rowley, and B. Lim. 1994. Cloning of the cDNA for a hematopoietic cell-specific protein related to CD20 and the β subunit of the high-affinity IgE receptor: evidence for a family of proteins with four membrane-spanning regions. *Proc. Natl. Acad. Sci. USA 91:10178.*
32. Kuster, H., L. Zhang, A. T. Brini, D. W. J. MacGlashan, and J.-P. Kinet. 1992. The gene and cDNA for the human high affinity immunoglobulin E receptor β chain and expression of the complete human receptor. *J. Biol. Chem. 267: 12782.*
33. Robbins, S. M., N. A. Quintrell, and J. M. Bishop. 1995. Myristoylation and differential palmitoylation of the HCK protein-tyrosine kinases govern their attachment to membranes and association with caveolae. *Mol. Cell. Biol. 15:3507.*
34. Garcia-Cardena, G., P. Oh, J. Liu, J. E. Schnitzer, and W. C. Sessa. 1996. Targeting of nitric oxide synthase to endothelial cell caveolae via palmitoylation: implications for nitric oxide signaling. *Proc. Natl. Acad. Sci. USA 93:6448.*
35. Dietzen, D. J., W. R. Hastings, and D. M. Lublin. 1995. Caveolin is palmitoylated on multiple cysteine residues: palmitoylation is not necessary for localization of caveolin to caveolae. *J. Biol. Chem. 270:6838.*
36. Oettgen, H. C., P. J. Bayard, W. Van Ewijk, J. M. Nadler, and C. P. Terhorst. 1983. Further biochemical studies of the human B-cell antigens B1 and B2. *Hybridoma 2:17.*
37. Tedder, T. F., and S. F. Schlossman. 1988. Phosphorylation of the B1 (CD20) molecule by normal and malignant human B lymphocytes. *J. Biol. Chem. 263: 10009.*
38. Valentine, M. A., T. Cotner, L. Gaur, R. Torres, and E. A. Clark. 1987. Expression of the human B-cell surface protein CD20: alteration by phorbol 12-myristate 13-acetate. *Proc. Natl. Acad. Sci. USA 84:8085.*
39. Valentine, M. A., K. E. Meier, S. Rossie, and E. A. Clark. 1989. Phosphorylation of the CD20 phosphoprotein in resting B lymphocytes: regulation by protein kinase C. *J. Biol. Chem. 264:11282.*
40. Clark, E. A., G. L. Shu, B. Luescher, K. E. Draves, J. Banchereau, J. A. Ledbetter, and M. A. Valentine. 1989. Activation of human B cells: comparison of the signal transduced by IL-4 to four different competence signals. *J. Immunol. 143:3873.*
41. Bubien, J. K., L. J. Zhou, P. D. Bell, R. A. Frizzell, and T. F. Tedder. 1993. Transfection of the CD20 cell surface molecule into ectopic cell types generates a Ca^{2+} conductance found constitutively in B lymphocytes. *J. Cell Biol. 121: 1121.*
42. Sargiacomo, M., P. E. Scherer, Z. Tang, E. Kubler, K. S. Song, M. C. Sanders, and M. P. Lisanti. 1995. Oligomeric structure of caveolin: implications for caveolae membrane organization. *Proc. Natl. Acad. Sci. USA 92:9407.*
43. Song, K. S., Z. Tang, S. Li, and M. P. Lisanti. 1997. Mutational analysis of the properties of caveolin-1: a novel role for the C-terminal domain in mediating homo-typic caveolin-caveolin interactions. *J. Biol. Chem. 272:4398.*
44. Mayor, S., K. G. Rothberg, and F. R. Maxfield. 1994. Sequestration of GPI-anchored proteins in caveolae triggered by cross-linking. *Science 264:1948.*